Geochemical Characteristic and Petrogenesis of Malumfashi Schist around Tandama Area, North-Western Nigeria

Idzi O. Alaku[1*], Ogunbajo I. Moshood[1], Ako T. Agbor[1] and Alabi A. Amos[1]

[1]*Department of Geology, Federal University of Technology Minna, Nigeria.*

Authors' contributions

This work was carried out in collaboration between all authors. Authors IOA and ATA designed the study, performed the statistical analysis, wrote the protocol and wrote the first draft of the manuscript. Authors ATA and OIM managed the analyses of the study. Author IOA managed the literature searches. All authors read and approved the final manuscript.

Original Research Article

ABSTRACT

Malumfashi schists which occur in association with migmatite-gneisses and biotite granite, occupy about 60% of Tandama area, north-western Nigeria. These rocks were studied with a view to evaluate their compositional characteristics and their evolution.

The lithology revealed from systematic mapping and petrographic examinations shows that the schist is mica schist, which is part of the Malumfashi Schist Belt of Nigeria. The mica schist consists of greater than 50% micaceous minerals and less than 50% quartz and feldspar. It is light grey to silver grey in colour, well foliated and mostly weathered to rusty brown or reddish brown. Mineralogical determinations from optical studies show a high proportion of biotite and minor amounts of plagioclase and quartz. Chemical analysis of the samples obtained by Inductively Coupled Plasma Mass Spectrometry (ICPMS) instrumentation method, involving major and trace elements reveals the nature of the mica schist. The A-CN-K diagram reveals a shale protolith which suffered moderate to high chemical weathering, prior to being metamorphosed. Obtained Rb/Sr ratio (>0.4%) and SiO_2/Al_2O_3 values support the shale protolith hypothesis for the schist, diagnostic

_____

*Corresponding author: E-mail: idzioramealaku@gmail.com;

geochemical features like the Na_2O/Al_2O_3 values, trace element ratios such as Th/U and REE patterns suggest that the protolith are predominantly derived from felsic igneous sources. Tectonically, SiO_2/Al_2O_3 versus K_2O/Na_2O plot revealed the protolith to have evolved within passive margin environment.

1. INTRODUCTION

The Basement Complex of Nigeria, which forms part of the Late Archean to early Proterozoic Pan-African mobile belt, is made up of three lithological units namely; the migmatite-gneisses, the schist belts and the Pan-Africa granites [1]. The schist belts occur dominantly in the western half of the Basement Complex of the country, exhibiting distinct petrological and structural features and they are made up of mainly low to medium grade metasediments. The schist belt form essentially north-south trending belts, composed largely of metamorphosed pelitic and psamitic assemblages.

The schists of the study area, which lies between latitudes 11°22' to 11°30'N and longitudes 07°23' to 07°30'E and covers a total area of 195 km^2, belong to the Malumfashi schist belt located in the NW of Nigeria. It is one of the twelve schist belts so far recognized in Nigeria, comprising basically of schists, migmatite-gneiss, quartzite, and Older granite with aplite and pegmatite forming minor lithologies. Malumfashi schist belt consists mainly of muscovite and biotite schist and phyllite interbedded with thin quartzites [2]. The pelitic rocks include minor graphitic and feldspathic schists, and contain frequent quartz and quartz-tourmaline veins. Interbedded quartzites are dominantly massive. Well-bedded quartzite units, sometimes several tens of metres thick, also occur. Minor rocks are spessartite quartzite, calc-silicate rocks and anthophyllite cordierite schist. Amphibolite form occasional discontinuous bands, with the largest occurrence being only approximately 12 m thick. The Malumfashi schist belt has been compared lithologically with the Kushaka schist belt [3]. But there are other important differences: (1) the quartzites are detrital and not chemically precipitated iron-silica formations; and (2) rocks of basic igneous composition are much less important. The rocks represent a fairly well differentiated sequence of muds and fine-grained sands. Structurally, the Malumfashi belt appears similar to the Zungeru-Birnin Gwari Schist belt, matching it closely in size and form [3].

Different models had been put forward for the evolution of the schist belts in Nigeria. McCurry [4] is in favour of the evolution of the schist belts through ensialic processes. [5] favoured the evolution through ensimatic processes, [6] and [7] suggested the formation of rift zones where sufficient extension led to the production of small basin. Holt [8] favoured formation through both ensialic and ensimatic. Geochemical features presented by [9] suggested the Kazaure Schist Belt to be of sedimentary origin, probably generated from the metamorphism of shale-greywacke.

The Malumfashi schist belt has been studied by [2,3] on a regional scale on the basis of petrography and not geochemistry. The research conducted by the Nigerian Geological Survey Agency (NGSA) has not been published yet. This study investigates the geochemical and petrogenetic features of part of Malumfashi schist belt, around Tandama area, in order to reconstruct its evolution.

2. MATERIALS AND METHODS

Field study and laboratory work constitute the research methodology. The field study involved of mapping of all the lithological units within the study area. The study was carried out utilizing rock exposures along roads and stream channels. Spatial relationship, texture and structural characteristics of the rock exposure were studied. A base map was used to mark the corresponding points where rocks occur in the field and were sampled. Detail observation of lithological contacts was also done by careful studying of areas in the field where lithologies change form one type to another.

In the laboratory, rock thin sections were prepared from representative rock samples collected from the field and the thin sections were prepared and used for petrographic studies. Both the thin section preparation and the petrographic study were done in the Department of Geology laboratory, Federal University of Technology, Minna, Nigeria.

Thirteen rock samples obtained from the field were taken to the Department of Geology and Mining, University of Jos, for sample preparation. The samples were broken into smaller pieces using geologic hammer, the smaller fragments were crushed and reduced to powder using FRITSCH Pulverisette 7. The powdered samples, pulverised to 8% passing 200 mesh, and measured to 5 g were transferred into labelled dispersing gloves for transportation to Acme laboratory at Vancouver, Canada, where the whole rock geochemical analyses were done using X-ray fluorescence (XRF) for major oxides and Inductively coupled plasma mass spectrometry (ICP-MS) for trace elements. For the XRF method, a predetermined amount of sample is roasted to determine the loss on ignition (LOI). The roasted sample is then fused in a platinum-gold crucible with a commercial lithium tetraborate (LiB_4O_7) flux. The molten material is cast in a platinum mold. Fused discs are then analyzed by XRF. For the ICP-MS method, prepared sample is digested with a modified Aqua Regia solution of equal parts concentrated HCl, HNO_3 and DI H_2O for one hour in a heating block or hot water bath. Sample is made up to volume with dilute HCl. After complete sample digestion, solution is read by an ICP-MS instrument to determine the trace element concentrations of the sample. The reported detection limits for the major oxides and trace elements are presented in Table 2.

3. RESULTS AND DISCUSSION

3.1 Lithology and Petrography

The study area comprises of migmatite-gneisses, schist and biotite granite. The migmatite-gneisses occupy the western part of the study area. The schists occupy the eastern part and cover half of the study area, and are intruded by the biotite granite in the southern part as shown in Fig. 1.

The mica schist is generally soft, fine to medium grained, strongly weathered and poorly exposed. It is exposed mostly along river channels and road cutting. It is extensive and constitutes about 60% of the entire study area; it is spatial contact with migmatite, granite gneiss, augen gneiss, and the intrusive biotite granite.

The schists fall within the class of pelitic schist. In hand specimen, the rocks consist of greater than fifty percent micaceous minerals and less than fifty percent quartz and feldspar. This mineral composition qualifies it to be mica schist. The schist is light grey to silver grey in colour, well foliated and mostly weathered to rusty brown or reddish brown. The pelitic schist generally shows a NE-SW orientation (strike) and with an average dip value of 54° W. Quartz veins within the pelitic schist are concordant and parallel to the original fabrics of the pelites, and are between 0.05 to 0.15 mm wide.

In thin section, quartz occurs as coarse-grained, stretched, and white to greyish anhedral blasts. Biotite occurs as light brown leaflet sometimes slender and prismatic with occasional stumpy laths and is pleochroic from light brown to reddish brown, showing alignment in the foliation plane (Fig. 2). The feldspar mineral grains present are mainly plagioclase and minor K-feldspar. The plagioclase displays a narrow albite twin lamellae characteristic of more sodic plagioclase, probably oligoclase. The K-feldspar is colourless and the crystal form is subhedral to anhedral displaying cross-hatched twinning, typical of microcline. They sometimes exhibit poikiloblastic texture and are characterized by inclusion of fine quartz and some mica. The quartz mineral grains vary in sizes from large to small (0.5 to 1.0 mm) in length with some having preferred orientation. There is widespread undulose extinction in the quartz grain.

3.2 Geochemistry

Whole-rock major and trace elements data of representative rock samples of the mica schists are represented in Table 1.

The mica schist displays a wide range in SiO_2 content 43.94 - 76.4 wt % (an average 66.97 w %), and high Al_2O_3 content in a range of 17.2 - 11.29 wt % (an average of 15.44 wt %). The Al_2O_3 content is higher and the K_2O content (1.81 - 6.64 wt %, an average of 4.37 wt %) is in excess of NaO content (0.01 - 0.43 wt %, an average 0.21 wt %). The high Al enrichment in the Al_2O_3 reflects the control of their composition by aluminous clay minerals. K_2O/Na_2O reflects probable secondary addition of potassium (K-metasomatism) during metamorphism [10]. The K_2O/Al_2O_3 ratios of terrigenous sedimentary rocks can be used as an indicator of the original composition of ancient sediments because K_2O/Al_2O_3 ratios for clay minerals and feldspars are different. K_2O/Al_2O_3 ratios for clay minerals range from 0.0 and 0.3 while that of feldspar range from 0.3 and 0.9 [11]. In the present study, the K_2O/Al_2O_3 ratio of the mica schist (0.43 ±

0.11) with majority falling within the 0.0 and 0.3 mark suggests that it contain considerable amounts of clay minerals. The SiO_2/Al_2O_3 values vary from 2.55 - 6.59 wt % (an average of 4.18 wt %), reflecting different degree of maturation of the metasediments, with those >5 wt % providing evidence of sedimentary maturation [12]. It has Fe_2O_3 content in the range of 2.43 - 14.63 wt % (average 5.60 wt %) and MgO content in range of 0.04 - 8.9 wt % (average 1.65 wt %), the MgO content is in excess of CaO content which is in the range of 0.01 - 0.24 wt % (average 0.097). Since MgO content is in excess of CaO content which is typically < 0.6 wt %, it is perhaps indicating the almost carbonate-free nature of the protolith [13]. The low Ca content results from the decomposition of plagioclase in the source material during weathering.
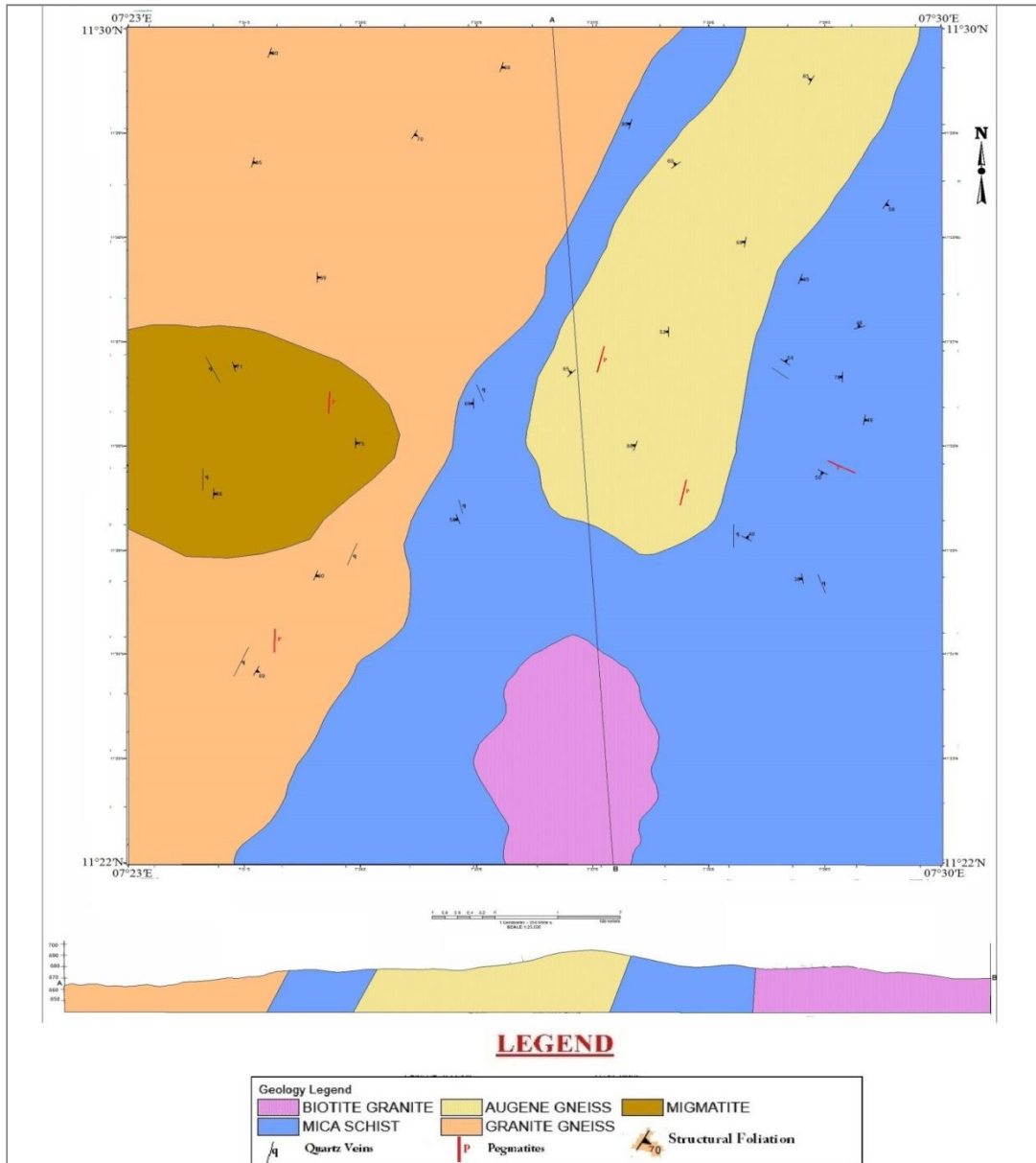
Fig. 1. Geological map and cross section of the study area

Table 1. Major and trace elements composition of mica schist

	ALA 3	ALA 5	ALA 7	ALA 8	ALA 9	ALA 10	ALA 11	ALA 12	ALA 13	ALA 16	ALA 19	ALA 20	ALA 22
Major oxides wt%													
SiO_2	74.42	75.09	70.83	62.89	76.4	75.82	68.72	72.03	70.02	43.94	62.93	57.68	59.89
Al_2O_3	11.29	13.36	15.41	19.26	12.76	12.77	16.77	16.13	15.51	17.2	17.09	17.08	16.13
Fe_2O_3	5.46	3.05	2.54	4.88	2.43	3.04	3.15	3.25	5.26	14.63	8.2	8.71	8.23
CaO	0.07	0.01	0.08	0.05	0.19	0.08	0.05	0.01	<0.01	0.18	0.03	0.24	0.17
MgO	1.09	0.28	0.39	0.64	0.22	0.34	0.56	0.16	0.23	8.9	1.51	3.15	3.95
Na_2O	0.24	0.1	0.43	0.25	1.02	0.15	0.22	0.02	0.05	0.07	0.04	0.19	0.01
K_2O	3.03	4.44	6.64	7.69	3.66	4.86	5.63	1.81	2.9	6.41	2.14	4.76	2.89
MnO	0.11	0.01	0.02	0.03	0.02	0.04	0.06	0.01	0.01	0.22	0.1	0.38	0.12
TiO_2	0.6	0.31	0.33	0.32	0.21	0.25	0.29	0.41	0.37	1.34	0.98	0.85	1.01
P_2O_5	0.08	0.03	0.04	0.01	0.03	0.04	0.03	0.05	0.09	0.04	0.05	0.04	0.04
Cr_2O_3	0.026	0.051	0.031	0.019	0.018	0.024	0.009	0.027	0.029	0.133	0.064	0.036	0.045
Total	96.416	96.731	96.741	96.039	96.958	97.414	95.489	93.907	94.469	93.063	93.134	93.116	92.485
Trace element (ppm)													
Ba	522	367	948	1164	834	660	679	262	424	813	631	957	513
Be	<1	2	2	9	4	2	4	2	<1	3	<1	6	2
Co	19.8	4.2	3.6	6	2.4	3.1	5.7	2.3	2.2	54.4	18.5	40.8	23.4
Cs	9.9	7.5	8.5	20.4	6.7	6.6	11.9	0.4	0.7	34.7	22.7	19.7	10.4
Ga	16.9	19.3	22.1	27.7	17.7	16	22.1	21.8	21.7	30.1	21.7	21.4	19.9
Hf	4.5	7.5	8.2	9.5	6.3	5.7	7.7	9.3	7.8	3	5.7	5.7	4.8
Nb	6.4	15.2	19.4	21.2	15.9	15.3	18.1	23	20.5	13.5	12.3	11.1	12.5
Rb	176.6	198.8	260.2	345.7	145.6	194	225.6	53.3	90.2	743.8	197.1	220.2	142.3
Sn	3	5	7	8	6	6	6	7	9	6	3	3	3
Sr	25.1	25.3	41.3	47.2	27.4	29.7	30.4	5.4	12.1	19.3	10.4	40.1	19.6
Ta	0.5	1.1	1.6	1.2	1.4	1.1	1.1	1.6	1.3	0.4	0.8	0.7	1.2
Th	7.8	18.2	25	26.5	17.8	16.2	24.1	19.9	20.4	5.5	10.8	11.5	7.8
U	2.6	1.7	4.3	3.6	4.3	2.4	4	2.8	4.4	6	4.9	2.8	4.1
V	103	18	17	17	<8	11	15	28	29	214	141	164	155
W	2.2	3.4	4.1	4.8	1.7	2.2	2.8	2.6	5.1	1.4	1.9	5.2	0.7
Zr	158	268.5	265.3	272.4	187.7	181.7	246.7	326.5	281.3	115.6	230.1	244.8	215.9
Y	28.7	46.4	65.6	33.1	71.1	49	64.6	84.4	111.7	17	74.5	31.7	43.1
La	34.7	36.4	68.5	30.6	63.9	50	70.1	54.2	36.6	36.2	54.4	41.2	27.9
Ce	93.9	89.9	117.8	66.7	142.8	100.4	117.8	99.7	66.1	110.5	64.3	188.3	54
Pr	7.87	10.36	15.43	8.42	14.43	12.46	17.36	21.56	11.17	8.28	19.21	9.49	7.63
Nd	30.5	45.9	61.2	34.9	57.5	49.1	67.5	94.4	46	32.9	88.1	39.3	34.3

						Samples							
	ALA 3	**ALA 5**	**ALA 7**	**ALA 8**	**ALA 9**	**ALA 10**	**ALA 11**	**ALA 12**	**ALA 13**	**ALA 16**	**ALA 19**	**ALA 20**	**ALA 22**
Sm	6.01	9.85	12.32	6.74	12.56	10.64	13.61	20.65	11.17	5.36	18.61	6.4	7.13
Eu	1.31	1.37	1.54	0.92	1.48	1.23	1.63	3.27	1.87	1.23	4.25	1.32	2.45
Gd	5.77	8.59	12.55	6.36	13.67	9.93	13.14	17.39	11.97	4.57	15.95	6.42	7.4
Tb	0.87	1.45	2.03	1.01	2.23	1.52	2.15	2.86	2.3	0.52	2.29	0.91	1.04
Dy	5.13	8.26	11.63	6.38	13.02	8.82	12.33	15.48	16.23	2.83	13.3	5.61	6.05
Ho	1.04	1.77	2.48	1.32	2.55	1.7	2.38	3.1	3.8	0.54	2.63	1.26	1.4
Er	3.06	4.99	6.92	4.05	7.99	5.99	7.03	8.62	12.49	1.69	7.15	3.59	3.77
Tm	0.46	0.84	1.01	0.62	1.1	0.81	1.03	1.28	1.92	0.24	1.08	0.57	0.54
Yb	2.96	5.52	6.48	4.38	6.89	5.31	6.51	8.37	12.25	1.54	7.24	3.64	3.28
Lu	0.45	0.84	0.95	0.65	1.04	0.8	0.95	1.22	1.84	0.27	1.05	0.55	0.53
Mo	3.1	3.6	2.4	1.9	1.2	2.9	0.6	0.7	1.7	0.9	1.4	1.1	1.3
Cu	34.4	11.7	11.6	19.9	7	16.4	5	11	21.7	46	47.2	58.6	31.4
Pb	8.5	2.3	5.1	8.7	14.2	6.8	9.8	4	5	38.2	18.7	28.8	20.2
Zn	88	2	25	62	11	24	32	5	18	284	125	110	150
Ni	49.2	121.2	68.8	39.8	25.9	46.8	9	20	33.3	293.2	107.3	78.1	136.2
LaN	53.55	56.17	105.71	47.22	98.61	77.16	108.18	83.64	56.48	55.86	83.95	63.58	43.06
CeN	56.06	53.67	70.33	39.82	85.25	59.94	70.33	59.52	39.46	65.97	38.39	112.42	32.24
PrN	30.98	40.79	60.75	33.15	56.81	49.06	68.35	84.88	43.98	32.6	75.63	37.36	30.04
NdN	24.4	36.72	48.96	27.92	46	39.28	54	75.52	36.8	26.32	70.48	31.44	27.44
PmN	NA	NA	NA	NA	NA	NA	NA	NA	NA	NA	NA	NA	NA
SmN	14.8	24.26	30.34	16.6	30.94	26.21	33.52	50.86	27.51	13.2	45.84	15.76	17.56
EuN	8.51	8.9	10	5.97	9.61	7.99	10.58	21.23	12.14	7.99	27.6	8.57	15.91
GdN	10.61	15.79	23.07	11.69	25.13	18.25	24.15	31.97	22	8.4	29.32	11.8	13.6
TbN	8.79	14.65	20.51	10.2	22.53	15.35	21.72	28.89	23.23	5.25	23.13	9.19	10.51
DyN	7.61	12.26	17.26	9.47	19.32	13.09	18.29	22.97	24.08	4.2	19.73	8.32	8.98
HoN	6.98	11.88	16.64	8.86	17.11	11.41	15.97	20.81	25.5	3.62	17.65	8.46	9.4
ErN	6.99	11.39	15.8	9.25	18.24	13.68	16.05	19.68	28.52	3.86	16.32	8.2	8.61
TmN	6.76	12.35	14.85	9.12	16.18	11.91	15.15	18.82	28.24	3.53	15.88	8.38	7.94
YbN	6.71	12.52	14.69	9.93	15.62	12.04	14.76	18.98	27.78	3.49	16.42	8.25	7.44
LuN	6.62	12.35	13.97	9.56	15.29	11.76	13.97	17.94	27.06	3.97	15.44	8.09	7.79
Eu/Eu*	0.68	0.45	0.38	0.43	0.34	0.37	0.37	0.53	0.49	0.76	0.75	0.63	1.03
LaN/YbN	7.98	4.49	7.19	4.75	6.31	6.41	7.33	4.41	2.03	16	5.11	7.7	5.79
LaN/SmN	3.62	2.32	3.48	2.84	3.19	2.94	3.23	1.64	2.05	4.23	1.83	4.03	2.45
GdN/LuN	1.6	1.28	1.65	1.22	1.64	1.55	1.73	1.78	0.81	2.12	1.9	1.46	1.75
EuN/YbN	8.35	4.29	4.79	4.01	5.46	4.98	4.76	3.14	1.42	18.89	2.34	13.62	4.33
CeN/YbN	3.79	2.21	2.32	2.4	2.76	2.29	2.1	1.17	1.43	5	0.84	7.13	1.84
CeN/SmN	1.27	0.71	0.68	0.6	0.62	0.66	0.72	1.12	0.44	2.29	1.68	1.04	2.14
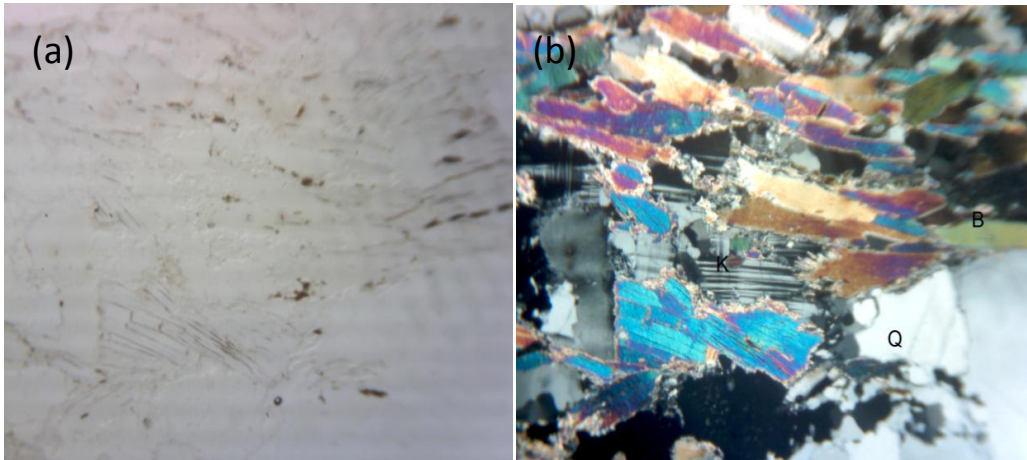
Fig. 2. Photomicrograph of Mica schist under (a) plane polarized light and (b) cross polarized light

B = Biotite, Q = Quartz, K = K-feldspar, Magnification = X10
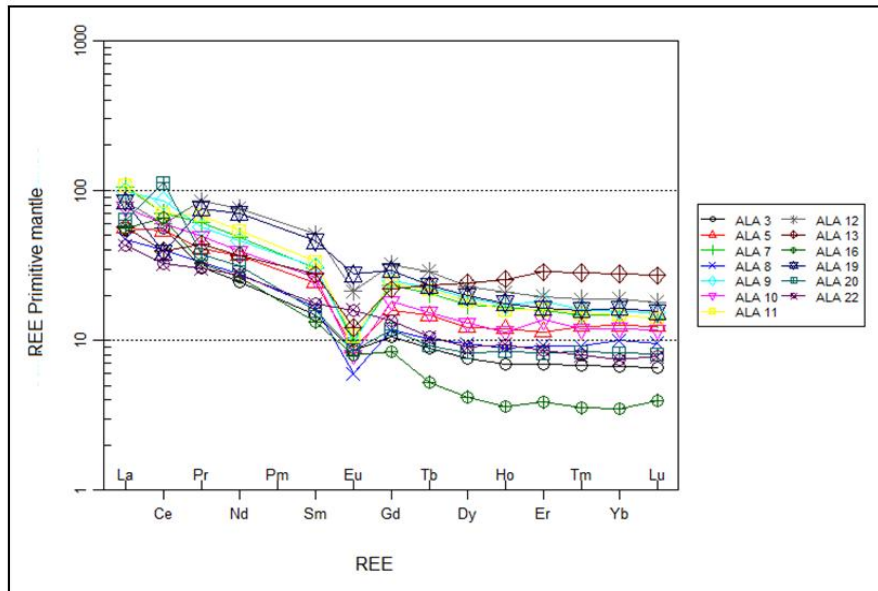
Fig. 3. The Rare Earth Elements (REE) spider plot (after [17]) of the mica schist displaying enrichment in LREE, a negative Eu anomaly and a flat HREE pattern

The mica schist has fairly high Ba in a range of 262 – 1164 ppm (an average of 674.92 ppm), Rb 90.2 - 743.8 ppm (an average 230.26 ppm), Zr 115.6 - 326.5 ppm (an average of 230.35 ppm). These concentrations are within the range of supracrustal rocks [14]. Zr concentration is a reflection of the presence of detrital zircon in the rock [15]. Sr content is in the range of 5.4 - 47.2 ppm (average 25.64 ppm). Zn (2-284 ppm, Average 72 ppm), Cu (5 - 58.6 ppm, Average 24.76 ppm), and Co (2.4 - 54.4 ppm, Average 14.34 ppm) concentration is low. The concentration of Rb is similar to their derivation from shales or metapelites, which is a reflection of their origin (pelite). Rb/Sr ratio which is >0.4 % is typical of pelitic metasediments [16], high Ba indicates K-feldspar rich source rock.

The patterns from the normalized REE Primitive mantle (after [17]) of the mica schists show gentle curves of decreasing relative abundances towards the heavy rare earth elements (HREEs) (Fig. 3). The light rare earth elements (LREEs) are enriched with distinct Eu anomalies.

Table 2. Detection limit for XRF (in wt %) and ICP-MS (in ppm, Au in ppb)

Element	Method detection limit
SiO_2	0.01wt%
Al_2O_3	0.01wt%
Fe_2O_3	0.01wt%
CaO	0.01wt%
MgO	0.01wt%
Na_2O	0.01wt%
K_2O	0.01wt%
MnO	0.01wt%
TiO_2	0.01wt%
P_2O_5	0.01wt%
Cr_2O_3	0.001wt%
Ba	1 ppm
Be	1 ppm
Co	0.2 ppm
Cs	0.1 ppm
Ga	0.5 ppm
Hf	0.1 ppm
Nb	0.1 ppm
Rb	0.1 ppm
Sn	1 ppm
Sr	0.5 ppm
Ta	0.1 ppm
Th	0.2 ppm
U	0.1 ppm
V	8 ppm
W	0.5 ppm
Zr	0.1 ppm
Y	0.1 ppm
La	0.1 ppm
Ce	0.1 ppm
Pr	0.02 ppm
Nd	0.3 ppm
Sm	0.05 ppm
Eu	0.02 ppm
Gd	0.05 ppm
Tb	0.01 ppm
Dy	0.05 ppm
Ho	0.02 ppm
Er	0.03 ppm
Tm	0.01 ppm
Yb	0.05 ppm
Lu	0.01 ppm
Mo	0.1 ppm
Cu	0.1 ppm
Pb	0.1 ppm
Zn	1 ppm
Ni	0.1 ppm
As	0.5 ppm
Cd	0.1 ppm
Sb	0.1 ppm
Bi	0.1 ppm
Ag	0.1 ppm
Au	0.5 ppb
Hg	0.01 ppm
Tl	0.1 ppm
Se	0.5 ppm

The HREEs are weakly fractionated with slight inclined to flat patterns. It has slightly high degree of LREE fractionation (($La/Yb)_N$ = 2.03 - 16) with weaker negative Eu anomalies (Eu/Eu* = 0.34 - 1.03). The mica schists have high La_N/Sm_N (1.64-4.23, an average of 2.91) and low Gd_N/Lu_N (0.81 - 2.12, Average 1.58) which is an indication of predominance of light REE over the heavy REE in the mica schist. The plot shows the curve to have a gentle trend with relative depletion of HREE relative to LREE.

3.3 Discussion

The petrogenetic character of the mica schist as indicated on the Na_2O/Al_2O_3 against K_2O/Al_2O_3 diagram (after Garrels and Mackenzie, [18]) shows the mica schist to be of sedimentary origin (Fig. 4), and thus has a sedimentary protolith. Sedimentary petrologists have shown that virtually all shales have lower Na_2O/Al_2O_3 values than the lowest limits for this ratio found in igneous rocks, whether mafic or felsic [18], as thus indicated in the plot.

The chemical composition of the mica schist provides insight into the nature of chemical weathering that gave rise to the source rock (shale). During weathering, large cations (Al_2O_3, Ba, Rb) remain fixed in the weathered residue in preference to smaller cations (Ca, Na, K, Sr) which are selectively leached [19]. These chemical signatures are ultimately transferred to the sedimentary record [20,21], thus providing a useful tool for monitoring source-area weathering conditions. During the initial stage of weathering, Na_2O and CaO are leached out from the earlier dissolved plagioclase. With increasing weathering intensity of the source rocks, the plagioclase are destructed which resulted in the loss of Ca and Na from plagioclase feldspar and the resulted sediments plot closer to the A-K axis of A-CN-K plot (Fig. 5). It is an indication that these sediments underwent intense chemical weathering in the source region. Those that follow the A-K trend line and plot between K-feldspar and muscovite fields imply that their source area experienced moderate intensity of chemical weathering. This typically shows that clay minerals are one of the major constituents of the source rock as represented in the A-CN-K diagram, which is characteristic of shale.

The chemical composition of the mica schist plotted in the ACF diagram (Fig. 6) points to shale protolith. The plot shows the mica schist falls in the fields of shale-graywackes [22], which suggest they originate from shale. This is confirmed in [23] who noted that the average composition of shale contains abundance of

Al_2O_3 and K_2O which is generally in excess of Na_2O. $K_2O>Na_2O$ is used to indicate shale, and high proportion of K-bearing rock forming minerals such as mica, K-feldspar, illite, compared to Na-feldspar which is unstable prior to metamorphism.
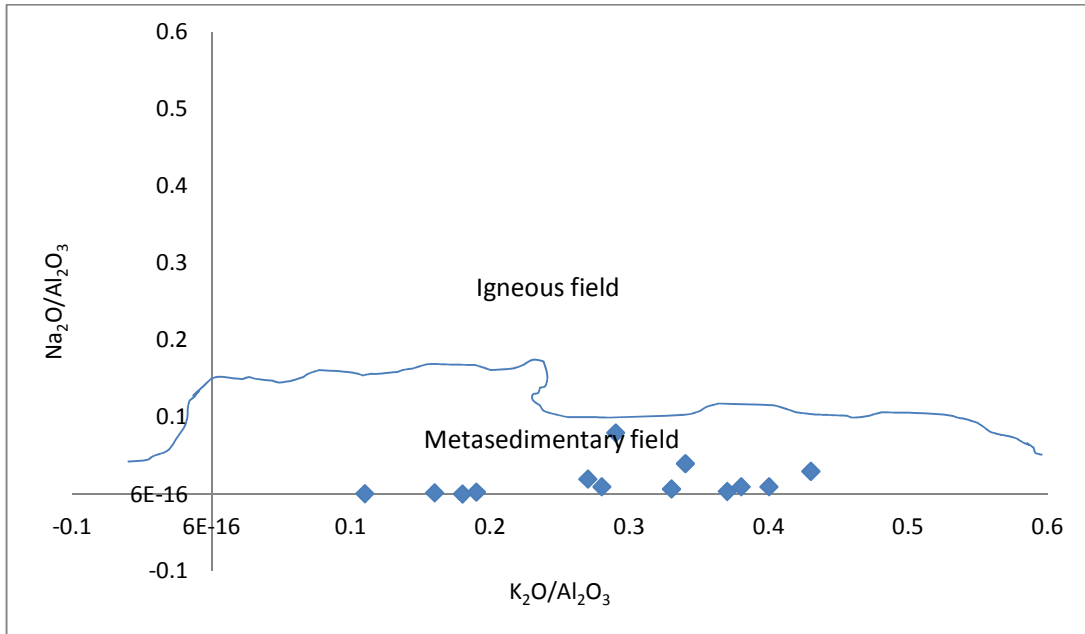
Fig. 4. Na_2O/Al_2O_3 versus K_2O/Al_2O_3 plot for the mica Schists of Tandama area (after [18])
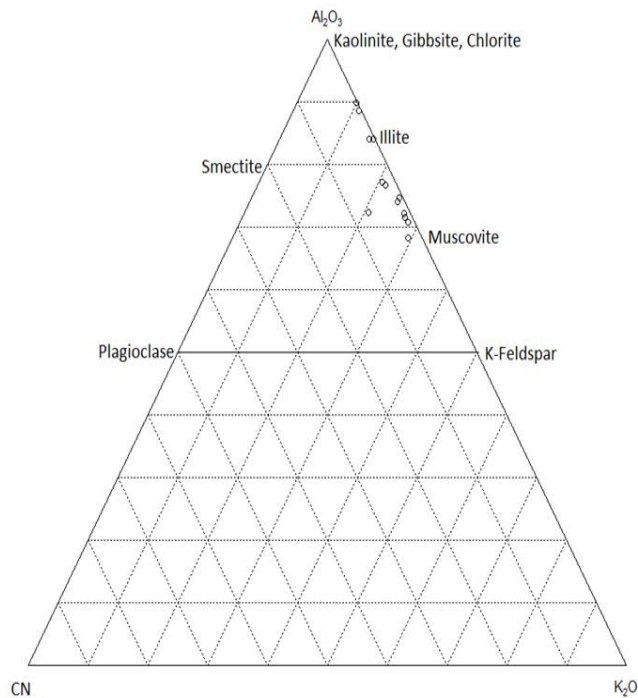
Fig. 5. A-CN-K diagram showing the weathering trend of the mica schist (after [20]).
A = Al_2O_3; CN = CaO + Na_2O; K = K_2O

$A=Al_2O_3 + Fe_2O_3 - Na_2O + K_2O$, $C=CaO$, $F=Fe_2O_3+MgO+MnO$
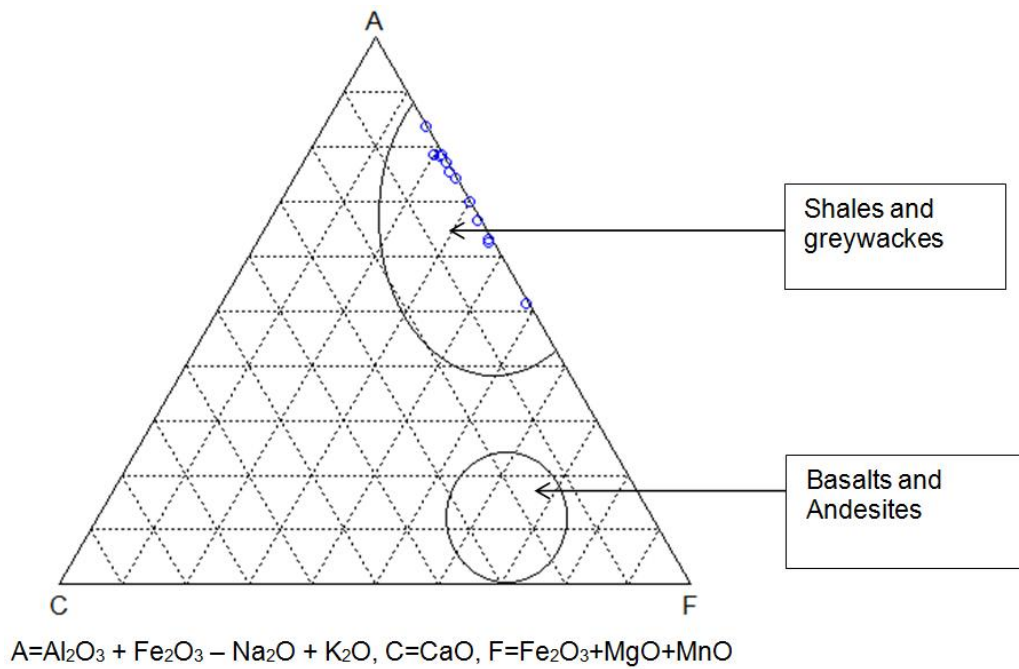
Fig. 6. Field of mica schist in the ACF diagram (after [22])
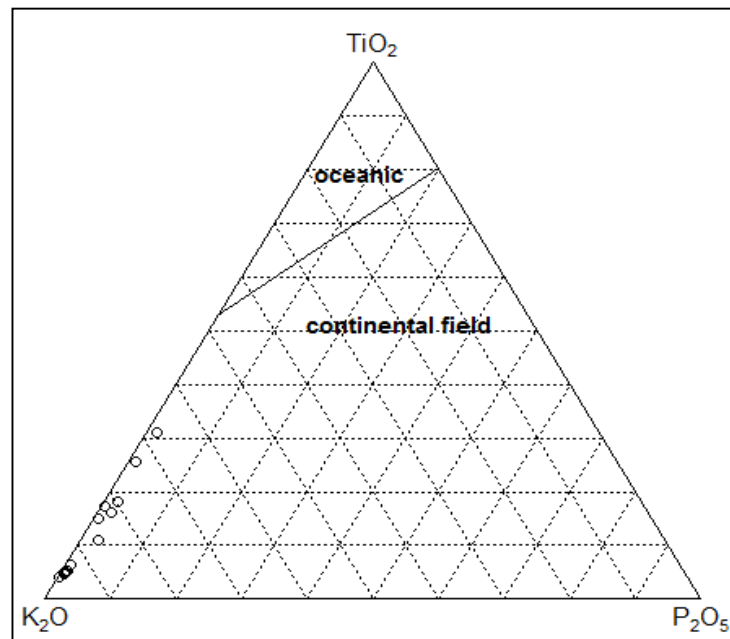
Fig. 7. TiO_2-K_2O-P_2O_5 diagram for the mica schist (after [24])

The TiO_2-K_2O-P_2O_5 plot (Fig. 7) (after [24]) of the mica schist confirms the continental nature of the sediments. The schist on the continental field is a confirmation of the continental nature of the sediments which underwent metamorphism. The geochemical signatures of clastic sediments have been used to determine their provenance [25-33]. Elements concentrated in mafic (Sc, Cr, and Co) and in silicic (La, Th, and REE) sediments, REE patterns, and the size
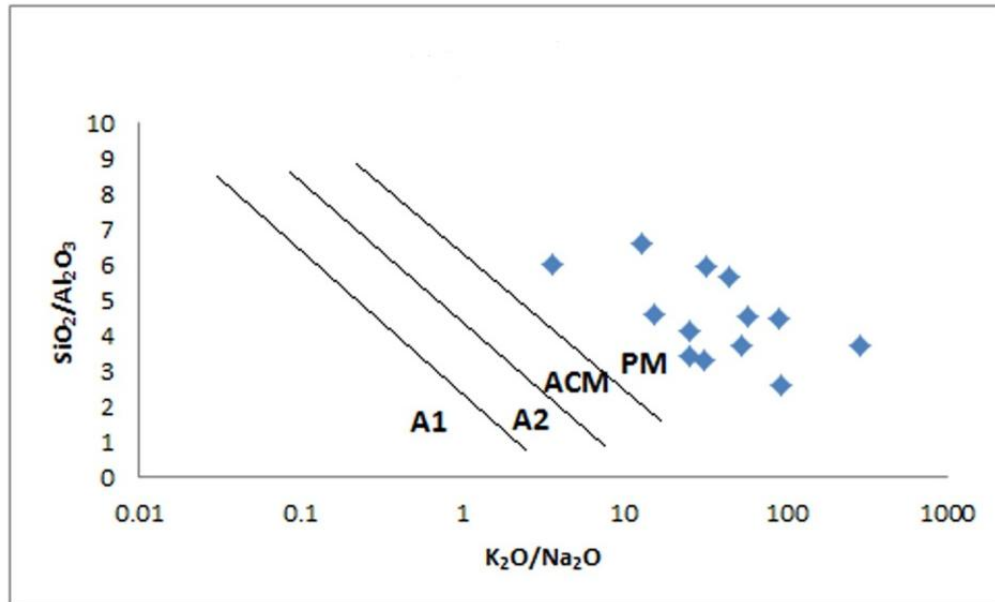
Fig. 8. SiO$_2$/Al$_2$O$_3$ versus K$_2$O/Na$_2$O plot of the rock samples of the study area
PM, passive margin; ACM, active continental margin; A1, arc setting, basaltic and andesitic detritus; A2, evolved arc setting, felsic–plutonic detritus

of the Eu anomaly have been used widely to understand the provenance signatures' interpretation [34]. The REEs and certain trace elements (Th, Sc, and Cr) can provide an insight into the provenance and are thus useful to constrain the average source-area composition [10,25,35-37].

Th/U ratio is also a useful parameter in determining the source characteristics of clastic sedimentary rocks [38]. This ratio ranges between 4.25- 4.30 in present day crust, while its values of 2.6 and 3.8 have been assigned to upper and lower mantle respectively [39]. Higher Th/U ratios can also increase in response to oxidative weathering and/or removal of U. Nevertheless, clastic sedimentary rocks derived from the upper crust are characterized by ratio ≥4, whereas ratio <4 has been related to a mantle contribution [38]. In the mica schist, Th/U ratio varies from 0.9–10.7(average 4.96). Most of the samples show high values of Th/U ratio of >4 which suggest that probably there have been significant proportion of the felsic rocks in the source region.

The REE patterns and the size of the Eu anomalies in the sediments provide useful information regarding source rock characteristics [25], because mafic igneous rocks have low LREE/HREE ratios and little or no negative Eu

anomalies, whereas felsic igneous rocks have higher LREE/HREE ratios and negative Eu anomalies [40,41]. In the present study, most of the sedimentary rocks show higher LREE/HREE ratios and negative Eu anomalies which suggest the felsic nature of the source rocks.

There is Eu depletion in the mica schist as indicated in the small negative Eu anomalies Eu/Eu* of 0.34 - 1.03 (Average 0.5). All post-Archean clastic sedimentary rocks of shale composition have negative Eu anomaly with average composition of Eu/Eu* = 0.66 of the upper crust [25]. Thus, the curves on the plot are similar to those of normalized REE of post-Archean shale known in the world [25,42, 43].

Taylor and McLennan [25] deduced that the absence of a Eu anomaly (Eu/Eu* = 1) or even the presence of local positive Eu anomaly indicate Archean sedimentary rocks. On the other hand, [44] ascribed the negative Eu anomaly in the clastic sedimentary rocks of post-Archean to detrital sources, during the formation of Eu depleted feldspar granites, after its formation by chemical fractionation. The Eu/Eu* values which is comparable between the mica schist in the study area and that of upper crust suggests the rocks were derived from similar source area with typical clay sediments.

Sandstone–mudstone suits from different tectonic settings can be distinguished on the basis of the K_2O/Na_2O and SiO_2/Al_2O_3 values and SiO_2 contents. On the SiO_2/Al_2O_3 versus K_2O/Na_2O plots (Fig. 8) [45], all samples of the mica schist plot in the passive continental margin. Thus, in terms of tectonic setting, the mica schists are of passive margin rocks.

4. CONCLUSION

Geochemical evaluation of part of Malumfashi schist belt around Tandama has revealed that the schist was generated from metamorphism of a shale protolith. A-CN-K plot reflects that the shale attained maturity and suffered moderate to intense chemical weathering before being subjected to metamorphism. Pattern of REE values, LREE and HREE characteristics, as well as Eu negative anomaly suggest considerable felsic component in the shale. Tectonic setting from the SiO_2/Al_2O_3 versus K_2O/Na_2O plot suggests the protolith to have evolved within passive margin environment.

COMPETING INTERESTS

Authors have declared that no competing interests exist.

REFERENCES

1. Elueze AA, Okunlola AO. Petrochemical and petrogenetic characteristics of Metasedimentary Rocks of Lokoja-Jakura Schist belt, Central Nigeria. Journal of Mining and Geology. 2003;39(11):21–27.
2. McCurry P. The Geology of the Precambrian to Lower Palaeozoic Rocks of Northern Nigeria–A Review. In: Kogbe CA, editor. Geology of Nigeria. Lagos: Elizabethan Publishers; 1976.
3. Grant NK. Structural distinction between a metasedimentary cover and an underlying basement in the 600 my old Pan-African domain of Northwestern Nigeria. Geol Soc Am Bull. 1978;89:50-58.
4. McCurry P. Pan-African orogeny in Northern Nigeria. Geological Society of America Bulletin. 1971;82(11):3251-3262.
5. Ajibade AC, Wright JB. The Togo-Benin-Nigeria shield: Evidence of crustal aggregation in Pan-African Belt. Tectonophysics. 1989;155:125–129.
6. Ogezi AEO. Geochemistry and geochronology of basement rocks north-western Nigeria. Unpublished Ph.D. Thesis, Leeds University United Kingdom. 1977;200- 207.
7. Bafor BE. The occurrence of sulphide mineralization in the Egbe area of South-western Nigeria. Journal of Mining and Geology. 1981;18(1):175-197.
8. Holt RW. The geotectonic evolution of the Anka Belt in the precambrian basement complex of NW Nigeria, PhD dissertation, Open University, Milton Keynes, UK. 1982;123-128.
9. Danbatta UA. Tectono-metamorphic evolution of the Kazaure Schist Belt, NW Nigeria. Paper presented at the-37" Annual Conference of Nigerian Mininig and Geoscience Society. NMGS Abtract. 2001; 33:56-109.
10. Fedo CM, Nesbitt HW, Young GM. Unraveling the effects of potassium metasomatism in sedimentary rocks and paleosols, with implications for paleoweathering conditions and provenance. Geology. 1995;23:921-924.
11. Cox R, Lowe DR. Controls on sediment composition on a regional scale: A conceptual view. Journal of Sedimentary Research. 1995;65:1-12.
12. Roser BP, Cooper RA, Nathan S, Tulloch AJ. Reconnaissance sandstone geochemistry, provenance and tectonic setting of the lower Paleozoic terranes of the West Coast and Nelson, New Zealand. New Zealand Journal of Geology and Geophysics. 1996;39(1):1-16.
13. Ekwueme BN. Petrology, geochemistry and Rb-Sr geochemistry of Uwet Area, South-eastern Nigeria. Unpublished PhD Thesis, University of Nigeria, Nsukka; 1985.
14. Brown EH, Babcock RS, Clark MD. Geology of Precambrian rocks of Grand Canyon: in petrology and structure of Vishu Complex. Precambrian Res. 1979;8(3-4):219-241.
15. Elueze AA. Dynamic metamorphism and oxidation of amphibolites of Tegina Area, North-western Nigeria. Precambrian Research. 1981;14(3):379-388.
16. Van de Kamp PC. Geochemistry and origin of metasediments in the Haliburton Modic area, south-eastern Ontario, Canada J. Earth Sci. 1968;5(6):1127-1136.
17. McDonough WF, Sun SS. The composition of the Earth. Chemical Geology. 1995; 120(3-4):223-253.

18. GarrelsRM, MacKenzie FT. Evolution of sedimentary rocks. W.W. Norton and Company, New York. 1971;394.

19. Nesbitt HW, Markovics G, Price RC. Chemical processes affecting alkalis and alkaline earth during continental weathering. Geochimica et Cosmochimica Acta. 1980;44(11):1659-1666.

20. Nesbitt HW, Young GM. Early Proterozoic climates and plate motions inferred from major element chemistry of lutites. Nature. 1982;299(5885):715-717.

21. Wronkijewicz DJ, Condie KC. Geochemistry of Archean shales from the Witwaters and super group, South Africa: source area weatheing and provenance. Geochimica et Cosmochimica Acta. 1987;51(9):2401-2416.

22. Miyashiro A. Metamorphism and metamorphic belts. George Allen & Unwin Ltd. London. 1973;492.

23. Pettijohn FJ. Sedimentary rocks. New York, Harper and Brothers. 2nd edition. 1957;718.

24. Pearce M, Gorman BE, Birkett TC. The Relationship between Major Element Chemistry and Tectonic Environment of basic and intermediate Volcanic Rocks. Earth and Planetary Science Letters. 1975; 36(1):121-132.

25. Taylor SR, McLennan SM. The continental crust: its composition and evolution. Oxford, Blackwell Scientific Publishing. 1985;312.

26. Cullers RL. The controls on the major and trace element evolution of shales, siltstones and sandstones of Ordovician to Tertiary age in the Wet Mountain region, Colorado, USA. Chemical Geology. 1995; 123(1-4):107-131.

27. Madhavaraju J, Ramasamy S. Petrography and geochemistry of late maastrichtian-early paleocene sediments of Tiruchirapalli Cretaceous, Tamil Nadu–Paleoweathering and provenance implications. Geological Society of India. 2002;59(2):133-142.

28. Armstrong-Altrin JS, Lee YI, Verma SP, Ramasamy S. Geochemistry of sandstones from the upper Miocene Kudankulam Formation, southern India: implications for provenance, weathering, and tectonic setting. Journal of Sedimentary Research. 2004;74(2):285-297.

29. Armstrong-Altrin JS, Nagarajan R, Madhavaraju J, Rosalez-Hoz L, Lee YI, Balaram V, Cruz-Martinez A, Avila-Ramirez G. Geochemistry of the jurassic and upper cretaceous shales from the Molango Region, Hidalgo, Eastern Mexico: Implications of source-area weathering, provenance, and tectonic setting. Comptes Rendus Geoscience. 2013;345(4):185–202.

30. Al-Juboury AI, Al-Hadidy AH. Petrology and depositional evolution of the Palaeozoic rocks of Iraq. Marineand Petroleum Geology. 2009;26(2):208–231.

31. Perri F, Critelli S, Mongelli G, Cullers RL. Sedimentary evolution of the Mesozoic continental redbeds using geochemical and mineralogical tools: The case of Upper Triassic to Lowermost Jurassic Monte di Gioiosa mudrocks (Sicily, southern Italy). International Journal of Earth Sciences. 2011;100(7):1569–1587.

32. Shadan M, Hosseini-Barzi M. Petrography and geochemistry of the Ab-e-Haji Formation in central Iran: Implications for provenance and tectonic setting in the southern part of the Tabas block. Rev Mex Cien Geol. 2013;30:80–95.

33. Madhavaraju J. Geochemistry of late cretaceous sedimentary rocks of the Cauvery Basin, South India: Constraints on paleo weathering, provenance and end Cretaceous environments. In: Ramkumar M, editor. Chemostratigraphy: Concepts, Techniques and Applications. 1st ed. Elsevier, the Netherlands. 2015;185-214.

34. Shynu R, Rao VP, Kessarkar PM, Rao TG. Rare earth elements in suspended and bottom sediments of the Mandovi estuary, central west coast of India: Influence of mining. Estuarine Coastal and Shelf Science. 2011;94(4):355-368.

35. Floyd PA, Shail R, Leveridge BE, Franke W. Geochemistry and provenance of Rhenohercynian synorogenic sandstones: Implications for tectonic environment discrimination. Geological Society London Special Publications. 1991;57(1):173–188.

36. McLennan SM, Hemming S, McDaniel DK, Hanson GN. Geochemical approaches to sedimentation, provenance and tectonics. Geological Society of America Special Papers. 1993;284:21-40.

37. Cullers RL, Berendsen P. The provenance and chemical variation of sandstones associated with the Mid-continent Rift System, USA. European Journal of Mineralogy. 1998;5:987-1002.

38. Roddaz M, Viers J, Brusset S, Baby P, Boucayrand C, Hérail G. Controls on

weathering and provenance in the Amazonian foreland basin: Insights from major and trace element geochemistry of Neogene Amazonian sediments. Chemical Geology. 2006;226(1):31-65.

39. Cullers RL, Podkovyrov VL. The source and origin of terrigenous sedimentary rocks in the Mesoproterozoic Ui group, Southeastern Russia. Precambrian Research. 2002;117(3):157–183.

40. Cullers RL. The chemical signature of source rocks in size fractions of Holocene stream sediment derived from metamorphic rocks in the Wet Mountains region, USA. Chemical Geology. 1994a; 113(3-4):327–343.

41. Cullers RL. The controls on the major and trace element variation of shale, siltstones, and sandstones of Pennsylvanian–Permian age from uplifted continental blocks in Colorado to platform sediment in Kansas, USA. Geochimica et Cosmochimica Acta. 1994b;58(22):4955–4972.

42. Haskin LA, Frey FA, Wilderman TR. Rare Earths in Sediments. Journal of Geophysical Research. 1960;71:6091-6105.

43. Martin JM, Meybeck M. Elemental mass-balance of material carried by major world rivers. Marine Chemistry. 1979;7(3):173-206.

44. Nance WB, Taylor SR. Rare earth element patterns and crustal evolution—II. Archean sedimentary rocks from Kalgoorlie, Australia. Geochimica et Cosmochimica Acta. 1977;41(2):225-31.

45. Roser BP, Korsch RJ. Determination of tectonic setting of sandstone-mudstone suites using SiO_2 content and K_2O/Na_2O ratio. The Journal of Geology. 1986; 94(5):635–650.

Peer-review history:
The peer review history for this paper can be accessed here:
http://sciencedomain.org/review-history/18564